Icarus 226 (2013) 1673–1677

Contents lists available at SciVerse ScienceDirect

Icarus

journal homepage: www.elsevier.com/locate/icarus

Temperature-dependent molecular absorption cross sections for exoplanets and other atmospheres

Christian Hill *, Sergei N. Yurchenko, Jonathan Tennyson

Department of Physics and Astronomy, University College London, Gower Street, WC1E 6BT London, UK

ARTICLE INFO

Article history:
Available online 14 August 2012

Keywords:
Atmospheres, Composition
Extrasolar planets
Infrared observations
Radiative transfer

ABSTRACT

Exoplanets, and in particular hot ones such as hot Jupiters, require very significant quantities of molecular spectroscopic data to model radiative transport in their atmospheres or to interpret their spectra. This data is commonly provided in the form of very extensive transition line lists. The size of these line lists is such that constructing a single model may require the consideration of several billion lines. We present a procedure to simplify this process based on the use of cross sections. Line lists for water, H_3^+, HCN/HNC and ammonia have been turned into cross sections on a fine enough grid to preserve their spectroscopic features. Cross sections are provided at a fixed range of temperatures and an interpolation procedure which can be used to generate cross sections at arbitrary temperatures is described. A web-based interface (www.exomol.com/xsecs) has been developed to allow astronomers to download cross sections at specified temperatures and spectral resolution. Specific examples are presented for water and ammonia.

1. Introduction

With the growing realization that many, probably most, stars support exoplanets, developing the means to systematically characterize the atmospheres of these planets has become a major scientific priority (Tinetti et al., 2012a). Given the likely complex chemistry of these atmospheres and the elevated temperature that is found in the most observable planets, there is a significant demand for spectroscopic data on the probable exoplanet atmospheric constituents.

Recently we have launched a new project, called ExoMol (see www.exomol.com), with the aim of providing molecular transition data appropriate for exoplanet models which are reliable over a wide range of temperatures (Tennyson and Yurchenko, 2012). The ExoMol project involves constructing line lists of spectroscopic transitions for key molecules which are valid over the entire temperature and wavelength domain that is likely to be astrophysically important for these species. Especially for polyatomic molecules, these line lists can become very large with hundreds of millions (Harris et al., 2006; Barber et al., 2006; Voronin et al., 2010; Tashkun and Perevalov, 2011) or even billions (Yurchenko et al., 2011) of individual transitions needing to be characterized and stored. A complete linelist for methane, for which so far only a preliminary version is available (Warmbier et al., 2009), can be expected to be even larger. Indeed potential line lists for larger species, such as higher hydrocarbons, for which spectroscopic data is needed for exoplanetary research, are likely to be so large as to potentially make their use impractical.

Molecular line lists are being actively used to model the spectra of exoplanets (e.g. Beaulieu et al., 2011) and cool brown dwarfs with similar temperatures (e.g. Lucas et al., 2010; Cushing et al., 2011). However, sampling billions of individual transitions to model relatively low resolution astronomical spectra is probably not necessary in many cases. An alternative approach is to represent the molecular absorptions as cross sections generated at an appropriate resolution and temperature. The advantage of this approach is that the data handling issues related to dealing with large data sets largely disappear. The disadvantage is that cross sections are inflexible – a particular cross section set is only valid for a single state of temperature and pressure. Cross sections are therefore often regarded as a second choice compared to maintaining a full line list (Rothman et al., 2009).

In this paper we develop a strategy whereby cross sections are provided for the user in a flexible fashion without significant loss of accuracy or the specificity of using a complete line list. To this end we have provided a web application which, starting from very high resolution cross sections generated for each molecule at a range of temperatures, can provide cross sections at a temperature and resolution specified by the user. Of course this approach is based on the implicit assumption of local thermodynamic equilibrium (LTE) and any non-LTE treatment will continue to have to rely on the explicit use of transition line lists. So far, these cross sections do not consider collisional broadening effects and are therefore, at their highest resolution, appropriate for the zero pressure limit only.

* Corresponding author.
E-mail address: christian.hill@ucl.ac.uk (C. Hill).

0019-1035/$ - see front matter © 2012 Elsevier Inc. All rights reserved.
http://dx.doi.org/10.1016/j.icarus.2012.07.028

The line lists for water (Barber et al., 2006; Voronin et al., 2010), H_3^+ (Neale et al., 1996; Sochi and Tennyson, 2010), HCN/HNC (Harris et al., 2002, 2006, 2008) and ammonia (Yurchenko et al., 2011) were used to generate cross sections for these species. For concreteness, this work uses the main water isotopologue, $H_2{}^{16}O$, as its working example. Water is known to be a key species in exoplanetary atmospheres and the BT2 line list has been used in studies of exoplanets (Tinetti et al., 2007, 2010a,; Swain et al., 2009; Baraffe et al., 2010; Shabram et al., 2011; Barman et al., 2011; Tessenyi et al., 2012) as well in a large variety of planetary (Bykov et al., 2008; Chesnokova et al., 2009; Bailey, 2009), astrophysical (Warren et al., 2007; Dello Russo et al., 2004, 2005; Burgasser et al., 2008; Barber et al., 2009; Lyubchik et al., 2007; Banerjee et al., 2005) and, indeed, engineering (Kranendonk et al., 2007; Lindermeir and Beier, 2012) studies which generally focus on the radiative transport by hot water. The BT2 line list was used as part of the recently updated HITEMP database (Rothman et al., 2010). In that work, the size of the line list was reduced using a technique based upon importance sampling at a range of key temperatures. In practice the number of water lines in HITEMP remains large, over 100 million.

The calculation of opacities and other spectral properties due to water vapour at these elevated temperatures can therefore become onerous, and so we present here pre-calculated absorption cross sections for a range of temperatures between 296 K and 3000 K, binned to different resolutions. The highest resolution cross sections are suitable for modelling low-density environments where only Doppler broadening contributes to the line width whereas by binning to a wavenumber grid spacing significantly larger than the pressure-broadened half-width, higher-density environments are described well by the calculated cross sections. However, no attempt is made to include contributions to the opacity from the water vapour continuum or water dimer absorption.

2. Method

The high-resolution cross section is calculated on an evenly-spaced wavenumber grid, $\tilde{\nu}_i$, defining bins of width $\Delta\tilde{\nu}$. Only Doppler broadening is considered so each absorption line has a Gaussian shape (Fig. 1):

$$f_G(\tilde{\nu};\tilde{\nu}_{0:j},\alpha_j)=\sqrt{\frac{\ln 2}{\pi}}\frac{1}{\alpha_j}\exp\left(-\frac{(\tilde{\nu}-\tilde{\nu}_{0:j})^2\ln 2}{\alpha_j^2}\right), \tag{1}$$

where the line centre position is $\tilde{\nu}_{0:j}$ and the Doppler half-width at half-maximum,

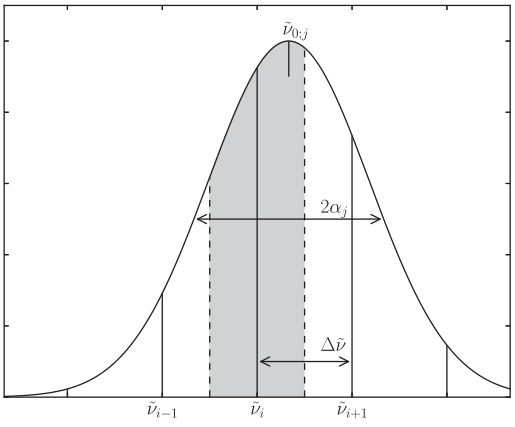

Fig. 1. The calculation of the absorption cross section in a wavenumber bin centred on $\tilde{\nu}_i$ due to a single line. The integrated line intensity within the shaded region, of width $\Delta\tilde{\nu}$, contributes to σ_{ij}.

$$\alpha_j=\sqrt{\frac{2k_BT\ln 2}{m}}\frac{\tilde{\nu}_{0:j}}{c}, \tag{2}$$

at temperature T for a molecule of mass m.

The contribution to the cross section within each bin is a sum over contributions from individual lines:

$$\sigma_i=\sum_j\sigma_{ij}, \tag{3}$$

where

$$\sigma_{ij}=\frac{S_j}{\Delta\tilde{\nu}}\int_{\tilde{\nu}_i-\Delta\tilde{\nu}/2}^{\tilde{\nu}_i+\Delta\tilde{\nu}/2}f_G(\tilde{\nu};\tilde{\nu}_{0:j},\alpha_j)\mathrm{d}\tilde{\nu}, \tag{4}$$

$$=\frac{S_j}{2\Delta\tilde{\nu}}\left[\mathrm{erf}\left(x_{ij}^+\right)-\mathrm{erf}\left(x_{ij}^-\right)\right], \tag{5}$$

where erf is the error function and

$$x_{ij}^{\pm}=\frac{\sqrt{\ln 2}}{\alpha_j}\left[\tilde{\nu}_i\pm\frac{\Delta\tilde{\nu}}{2}-\tilde{\nu}_{0:j}\right], \tag{6}$$

are the scaled limits of the wavenumber bin centred on $\tilde{\nu}_i$ relative to the line centre, $\tilde{\nu}_{0:j}$, and the line intensity in units of $\mathrm{cm}^{-1}/(\mathrm{molecule\ cm}^{-2})$ is

$$S_j=\frac{A_j}{8\pi c}\frac{g_j'\mathrm{e}^{-c_2E_j''/T}}{\tilde{\nu}_{0:j}^2Q(T)}(1-\mathrm{e}^{-c_2\tilde{\nu}_{0:j}/T}). \tag{7}$$

Here, g_j' and E_j'' are the upper-state degeneracy and lower-state energy respectively, A_j is the Einstein A coefficient for the transition and $c_2\equiv hc/k_B$ is the second radiation constant. For $H_2{}^{16}O$, the molecular partition function, $Q(T)$, was obtained from the tabulated values of Vidler and Tennyson (2000).

Note that in the limit of $\Delta\tilde{\nu}\gg\alpha_j$, Eq. (4) reduces to

$$\sigma_{ij}\approx\frac{S_j}{\Delta\tilde{\nu}}\int_{-\infty}^{+\infty}f_G(\tilde{\nu};\tilde{\nu}_{0:j},\alpha_j)\mathrm{d}\tilde{\nu}=\frac{S_j}{\Delta\tilde{\nu}}, \tag{8}$$

whereas for $\Delta\tilde{\nu}\ll\alpha_j$,

$$\sigma_{ij}\approx S_jf_G(\tilde{\nu}_i;\tilde{\nu}_{0:j},\alpha_j). \tag{9}$$

However, the exact expression is used in all calculations of the cross sections presented in this work.

3. Results

The absorption cross section of $H_2{}^{16}O$ was calculated between 10 cm^{-1} and 30,000 cm^{-1} across the temperature range 296–3000 K (Table 1), using the wavenumber grid-spacing given in Table 2. Each region was calculated to overlap with its neighbours by at least 1 cm^{-1}, which we find is sufficient to avoid discontinuities when they are binned to a common grid-spacing.

For comparison with experimental spectra, low-resolution cross sections were produced by binning the high-resolution cross sections to the following fixed grid spacing across the entire wavenumber range: $\Delta\tilde{\nu}=0.01,0.1,1,10,100\ \mathrm{cm}^{-1}$. At these resolutions, the structure due to individual lines is lost and direct comparison can be made with, for example, the experimental water vapour cross sections of the PNNL database (Sharpe et al., 2004). Such a comparison for the $\Delta\tilde{\nu}=10\ \mathrm{cm}^{-1}$ resolution spectra is shown in

Table 1
Temperatures at which calculated $H_2{}^{16}O$ cross sections are provided.

296 K	400 K	500 K	600 K
700 K	800 K	900 K	1000 K
1200 K	1300 K	1400 K	1600 K
1800 K	2000 K	2200 K	2400 K
2600 K	2800 K	3000 K	

Table 2
Summary of the grid spacings, $\Delta\tilde{\nu}$ for the cross sections calculated in different wavenumber regions.

Wavenumber range (cm^{-1})	$\Delta\tilde{\nu}$ (cm^{-1})
10–100	10^{-5}
100–1000	10^{-4}
1000–10,000	10^{-3}
10,000–30,000	10^{-2}

Fig. 2. We find excellent agreement between the calculated and measured spectra.

A similar comparison for the absorption cross section of ammonia in the region of its ν_2 vibration at 573 K is shown in Fig. 3. The cross section calculated from the variational, BYTe line list (Yurchenko et al., 2011) is compared to that calculated using the

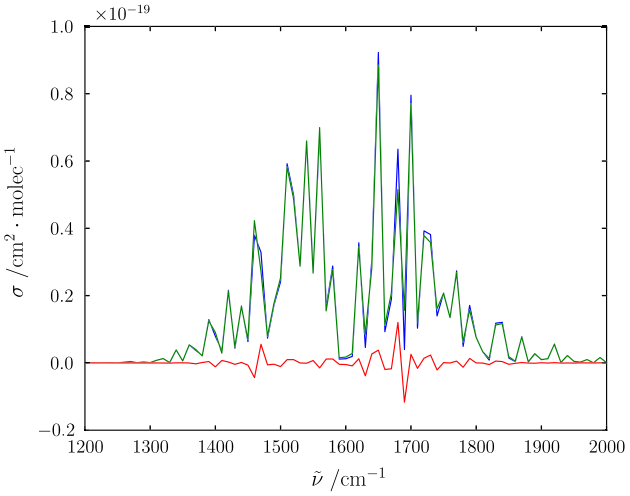

Fig. 2. Comparison of the calculated $H_2{}^{16}O$ cross section presented in this work (blue) with the experimental cross section of the PNNL database (Sharpe et al., 2004) (green) in the region of the fundamental ν_2 bending mode, at 296 K, both binned to a 10 cm^{-1} wavenumber grid. Also shown is the difference (this work – PNNL) between the two spectra (red). (For interpretation of the references to color in this figure legend, the reader is referred to the web version of this article.)

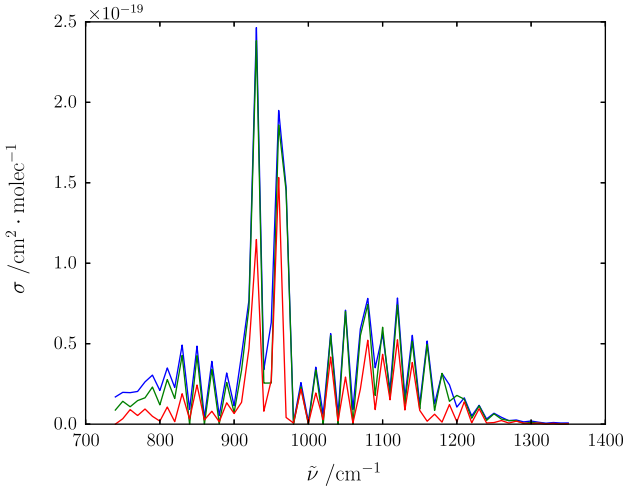

Fig. 3. Comparison of the calculated NH_3 cross section presented in this work (blue) with cross sections generated from the experimental line lists of Yu et al. (2010) (green) and Hargreaves et al. (2011) (red), in the region of the fundamental ν_2 normal mode, at 573 K, binned to a 10 cm^{-1} wavenumber grid. (For interpretation of the references to color in this figure legend, the reader is referred to the web version of this article.)

experimental line lists of Yu et al. (2010) and Hargreaves et al. (2011) for the one frequency region where the two measurements overlap. For a quantitative comparison, the integrated absorption cross sections over the wavenumber region 740–1350 cm^{-1} are 2.0×10^{-17} (BYTe), 1.8×10^{-17} (Yu et al.) and 0.9×10^{-17} cm/molecular (Hargreaves et al.). It can be seen that whilst agreement between our cross section and that of Yu et al. is generally good, the line list of Hargreaves et al. seems to underestimate the absorption in this region. It seems possible that at least some of this missing absorption is due to the contribution of a large number of weaker lines not included in the Hargreaves et al. data set, reabsorption of emitted radiation by ammonia in the cooler regions either side of their instrument's tube furnace, and the completion of that database with lines from the HITRAN 2008 database (Rothman et al., 2009), which is expected to be less accurate when used at higher temperatures.

4. Interpolation of cross sections between temperatures

For use in the web-based application described below, cross sections for the molecules given in Table 3 have been calculated using a wavenumber grid spacing of 0.01 cm^{-1} at a range of temperatures in 100 K intervals below 1000 K and 200 K intervals above 1000 K. A cross section at some intermediate temperature between the values at which the stored cross sections have been calculated may be obtained by interpolation. Suppose that $\sigma_i(T_1)$ and $\sigma_i(T_2)$ are calculated cross sections at temperatures which bracket the temperature of the desired cross section: $T_1 < T < T_2$ (we consider interpolation using only σ_i calculated at the two temperatures closest to T). One possible interpolation strategy is the linear interpolation

$$\sigma_i(T) = \sigma_i(T_1) + m(T - T_1), \quad \text{where } m = \frac{\sigma_i(T_2) - \sigma_i(T_1)}{T_2 - T_1}. \tag{10}$$

However, we find a more accurate approach is to estimate the temperature dependence to be of the form

$$\sigma_i(T) = a_i e^{-b_i/T}, \tag{11}$$

where the coefficients a_i and b_i at each wavenumber bin may be calculated from

$$b_i = \left(\frac{1}{T_2} - \frac{1}{T_1}\right)^{-1} \ln\frac{\sigma_i(T_1)}{\sigma_i(T_2)} \quad \text{and } a_i = \sigma_i(T_1)e^{b_i/T_1}. \tag{12}$$

The largest values of the interpolation residual error in the region 1000–20,000 cm^{-1}, calculated as $\delta\sigma_i = \sigma_{i,\text{calc}} - \sigma_{i,\text{interp}}$, are found to be associated with the ν_2 band – as an illustration, this is plotted in Fig. 4 at 350 K. The maximum value of the interpolation residual across this wavenumber region at a range of temperatures and wavenumber binning intervals is given in Table 4, expressed as a percentage of the corresponding absorption cross section:

$$\delta\sigma^{\%}_{\text{max}} = \max\left(\frac{|\sigma_{i,\text{calc}} - \sigma_{i,\text{interp}}|}{\sigma_{i,\text{calc}}}\right) \times 100. \tag{13}$$

Table 3
Summary of species for which cross sections are currently available. Also given for each species is the maximum wavenumber ($\tilde{\nu}_{\text{max}}$), the maximum temperature (T_{max}) and the reference to the original line list.

Species	$\tilde{\nu}_{\text{max}}$ (cm^{-1})	T_{max} (K)	Reference
H_3^+	10,000	4000	Neale et al. (1996)
H_2D^+	10,000	4000	Sochi and Tennyson (2010)
H_2O	20,000	3000	Barber et al. (2006)
HDO	17,000	3000	Voronin et al. (2010)
HCN/ HNC	10,000	4000	Harris et al. (2002, 2006)
$H^{13}CN$/ $H^{13}NC$	10,000	4000	Harris et al. (2008)
NH_3	12,000	1500	Yurchenko et al. (2011)

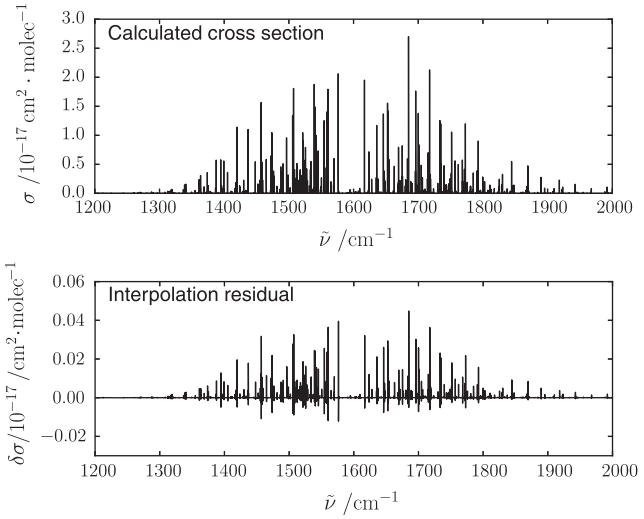

Fig. 4. Calculated $H_2^{16}O$ absorption cross section (upper pane) and interpolation residual (lower pane) in the region of the fundamental ν_2 bending mode, at 350 K, on a wavenumber grid spacing of 0.01 cm^{-1}. The interpolation residual error does not exceed 1.64%.

Table 4
Maximum interpolation errors in the $H_2{}^{16}O$ cross section as a function of wave number grid spacing and temperature.

$\Delta\tilde{\nu}$ (K)	0.01 cm^{-1} (%)	0.1 cm^{-1} (%)	1 cm^{-1} (%)	10 cm^{-1} (%)
350	1.64	1.34	1.07	1.10
1100	1.00	0.50	0.49	0.46
2500	0.66	0.40	0.37	0.36

In all cases, $\delta\sigma^{\%}_{\max}$ is found to be less than the estimated uncertainty in the *ab initio* line intensities that the cross section calculation is based on. Interpolation is performed on the 0.01 cm^{-1} grid before binning to a coarser wavenumber grid, if required.

Finally we note that Hargreaves et al. (2012) and Hargreaves et al. (submitted for publication) recently presented experimental spectra for ammonia and methane recorded at a range of temperatures at 100 K intervals. We suggest that our proposed interpolation scheme would also be appropriate for interpolating their data.

5. Web based application

Calculated absorption cross sections can be obtained from the interface at the url http://www.exomol.com/xsecs. The user of this web-based interface can select a wavenumber range, temperature and wavenumber grid spacing; using these parameters the interface software first obtains a high-resolution cross section at the desired temperature by the interpolation procedure described in the previous section on the pre-calculated spectra, and then bins this interpolated cross section to the requested wavenumber grid.

Cross sections are returned as a list of floating point numbers in a text file, separated by the Unix-style newline character, `LF` ('\n', `0x0A`). The wavenumber grid can be generated from the linear sequence

$$\tilde{\nu}_i = \tilde{\nu}_{\min} + i\Delta\tilde{\nu}; \quad i = 0, 1, 2, \ldots, n-1, \tag{14}$$

where the total number of points in the requested cross section is

$$n = \frac{\tilde{\nu}_{\max} - \tilde{\nu}_{\min}}{\Delta\tilde{\nu}} + 1. \tag{15}$$

We also provide an XML file in XSAMS format (Dubernet et al., 2009), compatible with the standards of the VAMDC project (Dubernet et al., 2010). This file may be thought of as a 'wrapper' to the cross section data, providing contextual metadata such as the molecular identity and structure, temperature of the calculation, and wavenumber limits and grid spacing. An example of the format is given in Table 5.

Table 5
Sample XSAMS format (Dubernet et al., 2009) XML wrapper for a cross section for $H_2{}^{16}O$ generated from 1000 to 20,000 cm^{-1} in steps of 1 cm^{-1} at a temperature of 296 K. In this example, the cross section itself is provided in the file `H2O_1000–20,000_296K-10.0.sigma` as a column of values, here in cm^2, one for each of 901 grid points.

```
<AbsorptionCrossSection envRef="EEXOMOL-1" id="PEXOMOL-XSC-
  1">
 <Description>
 The absorption cross section for H2O at 296.0 K, calculated at
 Sun Mar 11 19:50:45 2012, retrieved from www.exomol.com/xsecs
 </Description>
 <X parameter="nu" units="1/cm">
   <LinearSequence count="901" initial="1000."
  increment="10."/>
 </X>
 <Y parameter="sigma" units="cm2">
   <DataFile> H2O_1000–20,000_296K-10.0.sigma</DataFile>
 </Y>
 <Species>
   <SpeciesRef> XEXOMOL-XLYOFNOQVPJJNP-FNDQEIABSA-N</
  SpeciesRef>
 </Species>
 </AbsorptionCrossSection>
```

Cross section files have been generated for the polyatomic line lists currently available on the ExoMol website. These are listed in Table 3. The table also specifies the maximum wavenumber ($\tilde{\nu}_{\max}$) and maximum temperature ($T_{\max}$) for each species; we strongly caution against relying on the cross sections or indeed the underlying line lists at temperatures greater than those given. Further cross sections will be provided as line lists for new species become available.

6. Conclusion

High resolution absorption cross sections have been calculated for a number of molecules likely to be important in the atmospheres of exoplanets. The online interface provided at the ExoMol website (www.exomol.com) allows customized cross sections for a given molecular species to be returned at a specified temperature and resolution. Cross sections are only available for those species for which extensive line lists exist. New cross sections will be provided as further species are added to the ExoMol database; see Tennyson and Yurchenko (2012) for example.

It is our intention to make the cross section facility in ExoMol fully interoperable with other spectroscopic databases as part of the VAMDC (Virtual Atomic and Molecular Data Centre) project (Dubernet et al., 2010). Work in this direction will be reported in due course.

Finally we note that our current cross sections are all computed for zero pressure. Recent models have suggested that, particularly at long wavelengths, pressure broadening may be significant in exoplanets (Tinetti et al., 2012b). So far there is little data on broadening by appropriate species, notably H_2, at appropriate temperatures. However work in this direction is just started (Faure et al., 2012) and pressure effects on the cross sections will be considered if and when the necessary data becomes available.

Acknowledgments

We thank Giovanna Tinetti and Bob Barber for many helpful discussions during the course of this work. This work was

performed as part of ERC Advanced Investigator Project 267219 and the Project VAMDC which is funded by the European Union INFRA-2008-1.2.2 Scientific Data Infrastructure program under Grant Agreement Number 239108.

References

Bailey, J., 2009. A comparison of water vapor line parameters for modeling the Venus deep atmosphere. Icarus 201, 444–453.

Banerjee, D.P.K., Barber, R.J., Ashok, N.K., Tennyson, J., 2005. Near-infrared water lines in V838 Monocerotis. Astrophys. J. 672, L141–L144.

Baraffe, I., Chabrier, G., Barman, T., 2010. The physical properties of extra-solar planets. Rep. Prog. Phys. 73, 016901.

Barber, R.J., Miller, S., Dello Russo, N., Mumma, M.J., Tennyson, J., Guio, P., 2009. Water in the near IR spectrum of comet 8P/Tuttle. Mon. Not. R. Astron. Soc. 398, 1593–1600.

Barber, R.J., Tennyson, J., Harris, G.J., Tolchenov, R.N., 2006. A high accuracy computed water line list. Mon. Not. R. Astron. Soc. 368, 1087–1094.

Barman, T.S., Macintosh, B., Konopacky, Q.M., Marois, C., 2011. Clouds and chemistry in the atmosphere of extrasolar planet HR8799b. Astrophys. J. 733, 65.

Beaulieu, J.P. et al., 2011. Probing the atmosphere of the transiting hot Neptune GJ436b. Astrophys. J. 731, 18.

Burgasser, A.J., Liu, M.C., Ireland, M.J., Cruz, K.L., Dupuy, T.J., 2008. Subtle signatures of multiplicity in late-type dwarf spectra: The unresolved M8.5+T5 binary 2MASS J03202839-0446358. Astrophys. J. 681, 579–593.

Bykov, A.D. et al., 2008. Water vapor line width and shift calculations with accurate vibration–rotation wave functions. J. Quant. Spectrosc. Radiat. Trans. 109, 1834–1844.

Chesnokova, T.Y. et al., 2009. Calculation of solar radiation atmospheric absorption with different H_2O spectral line data banks. J. Mol. Spectrosc. 256, 41–44.

Cushing, M.C. et al., 2011. The discovery of Y dwarfs using data from the wide-field infrared survey explorer (WISE). Astrophys. J. 743, 50.

Dello Russo, N. et al., 2005. Water production rates, rotational temperatures and spin temperatures in comets C/1999 H1 (Lee), C/1999 S4 and C/2001 A2. Astrophys. J. 621, 537–544.

Dello Russo, N., DiSanti, M.A., Magee-Sauer, K., Gibb, E.L., Mumma, M.J., Barber, R.J., Tennyson, J., 2004. Accurate rotational temperature retrievals from hot-band line near 2.9 μm. Icarus 168, 186–200.

Dubernet, M.L. et al., 2010. Virtual Atomic and Molecular Data Centre. J. Quant. Spectrosc. Radiat. Trans. 111, 2151–2159.

Dubernet, M.L. et al., 2009. XSAMS: XML Schema for Atomic, Molecular and Solid Data, version 0.1. International Atomic Energy Authority. <http://www-amdis.iaea.org/xsams/documents/>.

Faure, A., Wiesenfeld, L., Drouin, B.J., Tennyson, T., 2012. Pressure broadening of water and carbon monoxyde transitions by molecular hydrogen at high temperatures. J. Quant. Spectrosc. Radiat. Trans., submitted for publication.

Hargreaves, R.J., Beale, C., Michaux, L., Irfan, M., Bernath, P.F., submitted for publication. Astrophys. J.

Hargreaves, R.J., Li, G., Bernath, P.F., 2011. Hot NH_3 spectra for astrophysical applications. Astrophys. J. 735, 111.

Hargreaves, R.J., Li, G., Bernath, P.F., 2012. Ammonia line lists from 1650 to 4000 cm^{-1}. J. Quant. Spectrosc. Radiat. Trans. 113, 670–679.

Harris, G.J., Larner, F.C., Tennyson, J., Kaminsky, B.M., Pavlenko, Y.V., Jones, H.R.A., 2008. A $H^{13}CN/HN^{13}C$ linelist, model atmospheres and synthetic spectra for carbon stars. Mon. Not. R. Astron. Soc. 390, 143–148.

Harris, G.J., Polyansky, O.L., Tennyson, J., 2002. Opacity data for HCN and HNC from a new *ab initio* linelist. Astrophys. J. 578, 657–663.

Harris, G.J., Tennyson, J., Kaminsky, B.M., Pavlenko, Y.V., Jones, H.R.A., 2006. Improved HCN/HNC linelist, model atmospheres and synthetic spectra for WZ Cas. Mon. Not. R. Astron. Soc. 367, 400–406.

Kranendonk, L.A. et al., 2007. High speed engine gas thermometry by Fourier-domain mode-locked laser absorption spectroscopy. Opt. Express 15, 15115–15128.

Lindermeir, E., Beier, K., 2012. HITEMP derived spectral database for the prediction of jet engine exhaust infrared emission using a statistical band model. J. Quant. Spectrosc. Radiat. Trans. 113, 1575–1593.

Lucas, P.W. et al., 2010. The discovery of a very cool, very nearby brown dwarf in the Galactic plane. Mon. Not. R. Astron. Soc. 408, L56–L60.

Lyubchik, Y. et al., 2007. Spectral analysis of high resolution near-infrared spectra of ultracool dwarfs. Astron. Astrophys. 473, 257–264.

Neale, L., Miller, S., Tennyson, J., 1996. Spectroscopic properties of the H_3^+ molecule: A new calculated linelist. Astrophys. J. 464, 516–520.

Rothman, L.S. et al., 2009. The HITRAN 2008 molecular spectroscopic database. J. Quant. Spectrosc. Radiat. Trans. 110, 533–572.

Rothman, L.S. et al., 2010. HITEMP, the high-temperature molecular spectroscopic database. J. Quant. Spectrosc. Radiat. Trans. 111, 2139–2150.

Shabram, M., Fortney, J.J., Greene, T.P., Freedman, R.S., 2011. Transmission spectra of transiting planet atmospheres: Model validation and simulations of the hot Neptune GJ436b for the James Webb Space Telescope. Astrophys. J. 727, 65.

Sharpe, S.W., Johnson, T.J., Sams, R.L., Chu, P.M., Rhoderick, G.C., Johnson, P.A., 2004. Gas-phase databases for quantitative infrared spectroscopy. Appl. Spectrosc. 58, 1452–1461.

Sochi, T., Tennyson, J., 2010. A computed line list for the H_2D^+ molecular ion. Mon. Not. R. Astron. Soc. 405, 2345–2350.

Swain, M.R. et al., 2009. Water, methane, and carbon dioxide present in the dayside spectrum of the exoplanet HD 209458b. Astrophys. J. 704, 1616–1621.

Tashkun, S.A., Perevalov, V.I., 2011. CDSD-4000: High-resolution, high-temperature carbon dioxide spectroscopic databank. J. Quant. Spectrosc. Radiat. Trans. 112, 1403–1410.

Tennyson, J., Yurchenko, S.N., 2012. ExoMol: Molecular line lists for exoplanet and other atmospheres. Mon. Not. R. Astron. Soc., in press, http://dx.doi.org/10.1111/j.1365-2966.2012.21440.x/abstract.

Tessenyi, M. et al., 2012. Characterising the atmospheres of transiting planets with a dedicated space telescope. Astrophys. J. 746, 45.

Tinetti, G. et al., 2012a. Exoplanet characterisation observatory. Exp. Astron..

Tinetti, G. et al., 2010b. Probing the terminator region atmosphere of the hot-Jupiter XO-1b with transmission spectroscopy. Astrophys. J. 712, L139–L142.

Tinetti, G. et al., 2010a. Exploring extrasolar worlds: From gas giants to terrestrial habitable planets. Faraday Discuss. 147, 369–377.

Tinetti, G., Tennyson, J., Griffiths, C.A., Waldmann, I., 2012b. Water in exoplanets. Philos. Trans. R. Soc. Lond. A 370, 2749–2764.

Tinetti, G. et al., 2007. Water vapour in the atmosphere of a transiting extrasolar planet. Nature 448, 169–171.

Vidler, M., Tennyson, J., 2000. Accurate partition function and thermodynamic data for water. J. Chem. Phys. 113, 9766–9771.

Voronin, B.A., Tennyson, J., Tolchenov, R.N., Lugovskoy, A.A., Yurchenko, S.N., 2010. A high accuracy computed line list for the HDO molecule. Mon. Not. R. Astron. Soc. 402, 492–496.

Warmbier, R., Schneider, R., Sharma, A.R., Braams, B.J., Bowman, J.M., Hauschildt, P.H., 2009. *Ab initio* modeling of molecular ir spectra of astrophysical interest: Application to CH_4. Astron. Astrophys. 495, 655–661.

Warren, S.J. et al., 2007. A very cool brown dwarf in UKIDSS DR1. Mon. Not. R. Astron. Soc. 381, 1400–1412.

Yu, S. et al., 2010. Submillimeter-wave and far-infrared spectroscopy of high-J transitions of the ground and $v_2 = 1$ states of ammonia. J. Chem. Phys. 133, 174317.

Yurchenko, S.N., Barber, R.J., Tennyson, J., 2011. A variationally computed hot (up to $T = 1500$ K) line list for NH_3. Mon. Not. R. Astron. Soc. 413, 1828–1834.